

Ultra-Lightweight Network for Ship-Radiated Sound Classification on Embedded Deployment

Sangwon Park, Dongjun Kim, Sung-Hoon Byun, Sangwook Park, *Member, IEEE*,

Abstract—This letter presents *ShuffleFAC*, a lightweight acoustic model for ship-radiated sound classification in resource-constrained maritime monitoring systems. *ShuffleFAC* integrates Frequency-Aware convolution into an efficiency-oriented backbone using separable convolution, point-wise group convolution, and channel shuffle, enabling frequency-sensitive feature extraction with low computational cost. Experiments on the DeepShip dataset show that *ShuffleFAC* achieves competitive performance with substantially reduced complexity. In particular, *ShuffleFAC* ($\gamma = 16$) attains a macro F1-score of $71.45 \pm 1.18\%$ using 39 K parameters and 3.06 M MACs, and achieves an inference latency of $6.05 \pm 0.95\text{ ms}$ on a Raspberry Pi. Compared with MicroNet0, it improves macro F1-score by 1.82% while reducing model size by $9.7\times$ and latency by $2.5\times$. These results indicate that *ShuffleFAC* is suitable for real-time embedded UATR.

Index Terms—UATR, Lightweight neural network, Embedded inference, frequency-adaptive convolution, channel shuffle

I. INTRODUCTION

WITH the rapid growth of maritime traffic, Underwater Acoustic Target Recognition (UATR), particularly ship-radiated sound classification, has become increasingly important for maritime surveillance, traffic monitoring, and marine environmental protection [1], [2]. In practical deployments, sensing platforms such as buoy networks and/or fixed hydrophone nodes operate continuously and autonomously under harsh ocean conditions. Reliable UATR on such platforms therefore requires acoustic models that are robust to ambient noise, reverberation, and diverse operating conditions. Recent deep learning-based approaches trained on large-scale real-world recordings consistently outperform traditional methods based on hand-crafted acoustic features [3], [4], [5].

However, on-device UATR remains challenging due to strict resource constraints. Power is typically supplied by batteries and energy harvesting, limiting the computational budget and duty cycle of onboard processing. Moreover, embedded hardware often relies on low-power CPUs or microcontrollers without high-performance GPUs, which restricts feasible model complexity. Memory and storage constraints further require careful control of model size. Despite these limitations, high recognition accuracy is essential because false alarms and missed detections can directly impact maritime safety and security. While Convolutional Neural Network (CNN)-



Fig. 1: Raspberry Pi 5: Resource-constraint platform

Transformer-based acoustic models achieve strong performance in high-resource settings, their parameter counts and compute demand often make direct deployment impractical on embedded UATR platforms [3], [6].

To address these constraints, resource-efficient network architectures are introduced for edge deployment on mobile and embedded platforms (Fig. 1). MobileNet employs separable convolution, decomposing a standard convolution into depth-wise and point-wise operations [7], [8]. Building on this idea, ShuffleNet adopts point-wise group convolution and channel shuffle to reduce computation while enabling cross-group information exchange [9], [10]. More recently, MicroNet further reduces complexity by introducing micro-factorized separable convolution [11]. Nevertheless, these models largely rely on shift-invariant convolution, which can be suboptimal for spectrogram-like inputs where frequency-axis position is informative [12]. Moreover, their practical efficiency on embedded devices can be affected by tensor-manipulation overhead (e.g., memory allocation and reshape/split operations) that is excluded in Multiply-Accumulate (MAC) counts [13].

This letter proposes *ShuffleFAC*, which combines frequency-aware feature extraction with an efficiency-oriented backbone to reduce both arithmetic cost and deployment overhead. Experiments on the *DeepShip* dataset, which contains underwater ship-radiated sound recordings, demonstrate that the proposed model achieves a favorable trade-off among classification performance, model size, MACs, and measured embedded inference latency. Specifically, with the channel scaling factor set to $\gamma = 16$, *ShuffleFAC* attains a macro F1-score of 71.45% using 39 K parameters and 3.06 M MACs, and runs in 6.05 ms on a Raspberry Pi 5. Compared with MicroNet0, it improves macro F1 by 1.82% while reducing model size by $9.7\times$ and inference latency by $2.5\times$.

Manuscript received December 1, 2025

Sangwon Park, Dongjun Kim, and Sangwook Park are with the Department of Electronic and Semiconductor Engineering, Gangneung-Wonju National University, Gangwon-do, 25457, Republic of Korea, e-mail: spark2@gwnu.ac.kr.(corresponding author). Sung-Hoon Byun is with Department of Ocean and Maritime Digital Technology Research, Korea Research Institute of Ships & Ocean Engineering, Daejeon, 34103, Republic of Korea

II. RELATED WORK

A. Separable convolution for Lightweight CNNs

Let $\mathbf{X} \in \mathbb{R}^{C_{in} \times H \times W}$ be an input feature map. A standard $k_h \times k_w$ convolution with C_{out} output channels requires $\mathcal{O}(HWk_hk_wC_{in}C_{out})$ operations and $k_hk_wC_{in}C_{out}$ parameters. Separable convolution reduces this cost by factorizing the operation into a depthwise convolution and a point-wise (1×1) convolution, resulting in $\mathcal{O}(HW(k_hk_wC_{in} + C_{in}C_{out}))$ operations and $C_{in}(k_hk_w + C_{out})$ parameters. This factorization forms the basis of MobileNet-style architectures for efficient on-device inference [7], [8].

ShuffleNet improves efficiency by using point-wise group convolution, reducing point-wise cost by approximately $1/g$ with g groups, and applies channel-shuffle to enable cross-group information exchange [9], [10]. MicroNet further reduces complexity through micro-factorization of spatial kernels and channel projections [11]. Specifically, the 2-D spatial kernel used in depthwise convolution is factorized as $p \otimes q^T$, where \otimes denotes outer product, $p \in \mathbb{R}^{k_h \times 1}$, and $q \in \mathbb{R}^{k_w \times 1}$. The weight matrix of the point-wise convolution is decomposed via an intermediate subspace as $\mathbf{W} = \mathbf{P}\phi\mathbf{Q}^T$, where $\mathbf{P} \in \mathbb{R}^{C_{in} \times C_{int}}$, $\phi \in \mathbb{R}^{C_{int} \times C_{int}}$, and $\mathbf{Q} \in \mathbb{R}^{C_{out} \times C_{int}}$ [11]. With these factorizations, micro-factorized separable convolution reduces the MAC count to $\mathcal{O}((Hk_h + Wk_w)C_{in} + HWC_{int}(C_{in} + C_{out}))$ and the number of parameters to $C_{in}(k_h + k_w) + C_{int}(C_{in} + C_{out})$. While these approaches reduce arithmetic cost, practical embedded latency can still be influenced by tensor manipulations (e.g. tensor split, slice, copy) and memory movement beyond MAC counts.

B. Frequency Adaptive Convolution

In time-frequency representations, the same local pattern can convey different semantics depending on its frequency band. Frequency-adaptive convolution incorporates frequency-position information so that the effective filtering can vary along the frequency axis.

Frequency dynamic convolution typically achieve frequency adaptivity by combining multiple frequency-conditioned kernels [14]. Because it evaluates and aggregates responses from multiple kernels, its computational and parameter costs scale with the number of basis kernels. In contrast, Frequency Aware Convolution (FAC) injects frequency-position information using a positional encoding and lightweight channel-wise modulation prior to convolution [12]. FAC achieve frequency sensitivity without requiring multiple kernel evaluations, making it attractive for embedded deployment.

III. PROPOSED METHOD

When designing an acoustic model for embedded UATR, the top priority is to achieve both computational efficiency and strong classification accuracy. To this end, the proposed model is designed by combining frequency-aware feature extraction with an efficiency-oriented backbone.

A. Frequency Adaptive Separable Convolution Module

Fig. 2(a) illustrates a diagram of Frequency-Adaptive Separable Convolution (FASC) module, which integrates

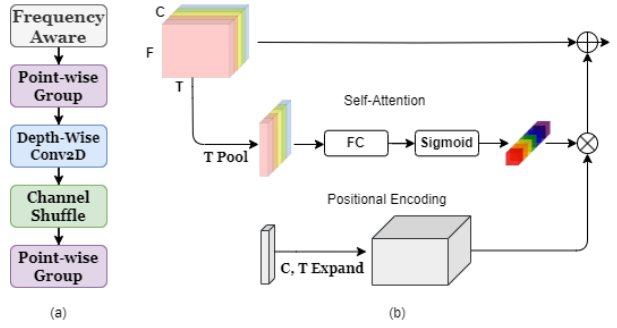


Fig. 2: Illustrations of (a) Frequency Adaptive Separable Convolution module, (b) Frequency aware pipeline

a frequency-aware (FA) block into an efficiency-oriented separable-convolution. The FA block injects frequency-position information through a learnable positional encoding (Fig. 2(b)). Specifically, the encoding is broadcast along the time and channel dimensions to match the input feature-map shape and is modulated by channel-wise gates produced by a lightweight self-attention branch (temporal pooling, a Fully-Connected (FC) layer, and sigmoid activation). The resulting channel-weighted positional bias is then added to the input feature map. This design enables frequency-sensitive feature extraction with only mild overhead, since it relies primarily on element-wise operations and a matrix multiplication rather than additional convolutional kernels. Because the injected bias is constant over time, the FA block is particularly effective for quasi-stationary signals, which is consistent with ship-radiated sound characteristics.

A ShuffleNet-style separable block requires approximately $\mathcal{O}(HWk_hk_wC_{in}^2 + 2HWC_{in}^2/g)$ operations when the output channel is doubled ($C_{out} = 2C_{in}$). In this setting, the depthwise term typically dominates the total complexity because $k_hk_w > 2/g$. To mitigate this issue, channel compression is applied prior to the depthwise convolution. Specifically, after the FA block, a point-wise group convolution (with $g_1 = 2$) reduces the channel dimension by a factor of two, followed by a depthwise convolution for spatial feature extraction at the reduced channels. Channel shuffle is then applied to enable cross-group information exchange, and a second point-wise group convolution (with $g_2 = 2$) expands the channels to twice the input channel for the subsequent stage. Notably, increasing the number of groups reduces the MACs of point-wise group convolution, but it can also introduce additional tensor-manipulation overhead that degrades practical latency on embedded CPUs.

B. ShuffleFAC Architecture

For embedded UATR, a lightweight acoustic model is designed by stacking the proposed FASC modules with ReLU activation, Batch Normalization (BN), and Average pooling (AvgPool), as summarized in Table I. Given a log-Mel spectrogram with 128-frequency bands and 24-frames as the input tensor $\mathbf{X} \in \mathbb{R}^{1 \times 128 \times 24}$, the first stage applies the FA block and a standard convolution from [12] to perform initial channel expansion to γ . Subsequent layers employ the FASC module for efficient frequency-adaptive feature extraction, where the

TABLE I: Proposed Model Architecture

Stage	Configuration	Output Shape
Input	Log-mel spectrogram	$1 \times 128 \times 24$
Channel Expansion	FA, Conv2D (γ), ReLU, BN, AvgPool (2×2)	$\gamma \times 64 \times 12$
	FASC (2γ), ReLU, BN, AvgPool (2×2)	$2\gamma \times 32 \times 6$
	FASC (4γ), ReLU, BN, AvgPool (1×2)	$4\gamma \times 16 \times 6$
	FASC (8γ), ReLU, BN, AvgPool (1×2)	$8\gamma \times 8 \times 6$
Feature Embedding	FASC (8γ), ReLU, BN, AvgPool (1×2)	$8\gamma \times 4 \times 6$
	FASC (8γ), ReLU, BN, AvgPool (1×2)	$8\gamma \times 2 \times 6$
	FASC (8γ), ReLU, BN, AvgPool (1×2)	$8\gamma \times 1 \times 6$
Classifier	Global AvgPool, Linear (8γ , 4)	4

channel is progressively doubled up to the fourth stage, while later stages keep the channel dimension fixed.

Average pooling is used to down-sample the frequency dimension throughout the network, while the time dimension is reduced mainly in the first two stages. This channel and pooling configuration reduces the overall computational cost of separable convolution. Moreover, unlike MobileNetV2 [8] and ShuffleNetV2 [10], the proposed architecture avoids residual and parallel paths, thereby reducing tensor-manipulation overhead that can degrade practical latency on embedded processors. Finally, global average pooling is applied to the final feature map, and a linear layer projects the pooled feature vector to the target class space.

C. Model Training

The model parameters are optimized using mini-batch stochastic gradient descent by minimizing the Cross-Entropy (CE) loss

$$\mathcal{L}_{\text{CE}}(y, \hat{y}) = -\frac{1}{N} \sum_{n=1}^N \sum_{c=1}^C y_{n,c} \log(\hat{y}_{n,c}), \quad (1)$$

where N and C denote the number of samples in a mini-batch and the number of target classes, respectively. Here, $y_{n,c}$ is the one-hot ground-truth label and $\hat{y}_{n,c}$ is the model's prediction that the n th sample belongs to class c . During the training, Adam optimizer with a learning rate of 0.001 is applied under the setting of batch size 48 ($N = 48$) and a maximum of 200 epochs¹.

IV. EXPERIMENTS

A. Database and Pre-processing

Experiments are conducted on the DeepShip dataset, which contains approximately 47 h of real-world underwater record-

ings from 265 ships across four vessel categories [3]. To construct non-overlapping subsets, the original recordings are split at the file level into training, validation, and test sets with a ratio of 7:1:2. Each recording is resampled to 16 kHz and segmented into 3-s audio clips without overlaid. This procedure yields approximately 56,000 clips. Because segmentation is performed after the file-level split, all clips from a given recording are assigned to a single subset, preventing train-test contamination and better reflecting performance on unseen recordings. Each 3-s clip is converted into a log-Mel spectrogram by computing the short-time Fourier transform with a 256-ms window and 128-ms hop, taking the magnitude, applying a 128-channel Mel filterbank, and then performing log-amplitude scaling.

B. Evaluation Metrics and Experimental Settings

This study compares the proposed model with representative lightweight architectures adapted to the DeepShip-based UATR task by making minor modifications to their input/output layers and pooling settings. Specifically, FAC, Separable Convolution based Autoencoder (SCAE), MobileNet, ShuffleNet, and MicroNet are considered as baseline models. All models are trained and evaluated on a high-resource workstation equipped with an NVIDIA RTX A5000 GPU.

In the assessment, two types of metrics are used to evaluate classification accuracy and efficiency. For classification, micro *Accuracy* and macro *F1-score* are reported. Accuracy is computed at the clip level, while macro F1-score is obtained by averaging the classwise F1-scores. The F1-score is the harmonic mean of precision and recall, where a correct prediction contributes one true positive and an incorrect prediction contributes one false positive and one false negative. A small gap between Accuracy and F1-score indicates more balanced performance across targets. Each assessment is repeated at least three times, and the results are reported as the mean and standard deviation.

To assess efficiency, the number of trainable parameters and MACs are reported as measures of model size and computational complexity. In addition, inference latency of each model is measured on a Raspberry Pi 5 with 8 GB RAM to capture practical overhead from tensor manipulation that is excluded in MAC counts (Fig. 1). Finally, the energy consumption per inference is estimated from the measured inference time under an assumed CPU utilization of 90% as $E_{\text{est}} = 0.9P_{\text{cpu}} \times t_{\text{inf}}/3600$, where P_{cpu} is the CPU peak power in Watts and t_{inf} is the inference time in seconds.

C. Results

Table II summarizes the classification performance and model complexity of all models. For most architectures, micro Accuracy and macro F1-score are close, indicating relatively balanced performance across the vessel categories rather than strong bias toward a subset of classes. As two benchmarks, FAC and SCAE achieve strong classification performance as Accuracy: $72.85 \pm 1.90\%$ and $72.37 \pm 1.18\%$, respectively. However both are less suitable for embedded deployment due to their high computational cost and latency. In particular,

¹Online available: <https://github.com/KNU-LMAP/ShuffleFAC>

TABLE II: Comparison of performance each models

Model	Accuracy (%)	F1-score (%)	# of Params	MACs	t_{inf} (ms)	E_{est} (μWh)
*FAC	72.85 ± 1.90	73.12 ± 2.14	2.45 M	129.25 M	13.97 ± 1.13	34.92 ± 2.83
*SCAE	72.37 ± 1.18	72.59 ± 1.25	1.53 M	560.03 M	45.22 ± 0.66	113.05 ± 1.66
MobileNet	70.55 ± 0.64	70.85 ± 0.74	3.22 M	40.99 M	14.69 ± 3.05	36.71 ± 7.63
MobileNetV2	68.92 ± 0.02	69.42 ± 0.20	2.25 M	28.70 M	13.95 ± 0.78	34.88 ± 1.96
ShuffleNet	69.17 ± 3.37	69.46 ± 3.48	919 K	10.48 M	13.70 ± 0.56	34.25 ± 1.41
ShuffleNetV2	69.58 ± 1.25	69.91 ± 0.13	1.26 M	10.73 M	11.02 ± 0.49	27.55 ± 1.23
MicroNet 3	70.40 ± 0.77	70.81 ± 0.78	1.60 M	3.32 M	23.05 ± 0.92	57.64 ± 2.31
MicroNet 2	69.55 ± 1.13	70.11 ± 1.09	1.37 M	2.27 M	23.67 ± 1.50	59.18 ± 3.77
MicroNet 1	68.75 ± 1.09	69.33 ± 1.07	818 K	1.21 M	16.23 ± 1.77	40.58 ± 4.44
MicroNet 0	69.04 ± 0.46	69.63 ± 0.50	379 K	0.65 M	15.13 ± 1.26	37.82 ± 3.16
ShuffleFAC ($\gamma = 64$)	70.26 ± 0.52	70.17 ± 0.79	546 K	34.64 M	10.86 ± 0.84	27.16 ± 2.11
ShuffleFAC ($\gamma = 32$)	71.44 ± 1.71	71.66 ± 1.74	143 K	9.85 M	7.49 ± 1.31	18.73 ± 3.29
ShuffleFAC ($\gamma = 16$)	71.31 ± 1.34	71.45 ± 1.18	39 K	3.06 M	6.05 ± 0.95	15.14 ± 2.37
ShuffleFAC ($\gamma = 8$)	69.15 ± 1.46	69.38 ± 1.67	11 K	1.06 M	5.48 ± 0.70	13.71 ± 1.77

*our implementation

SCAE exhibits the largest MACs and the highest inference time on Raspberry Pi, which is consistent with its Xception-style design that stacks multiple separable convolutions with residual connections, which increases both operations and runtime overhead [15].

Conventional lightweight architectures reduce model complexity at the expense of recognition performance. MobileNet decreases the MACs substantially relative to FAC (129.25 $M \rightarrow 40.99 M$) with moderate performance degradation, while MobileNetV2 further reduces MACs and parameters but shows additional degradation in both Accuracy and F1. ShuffleNet and ShuffleNetV2 operate in the $\sim 10 M$ MACs and achieve improved embedded latency as 13.70 ± 0.56 ms and 11.02 ± 0.49 ms, respectively. But their performance remains below MobileNet. MicroNet variants achieve extremely low MACs (down to 0.65 M for MicroNet0), but their classification performance still remains at the level of the MobileNets. Also, their measured latency still remains relatively high about $15 \sim 23$ ms, suggesting that practical runtime on embedded platform is influenced by factors beyond MACs, such as memory access and tensor-operator overhead. This issue is analyzed in more detail in the next section.

The proposed ShuffleFAC models provide a favorable accuracy-efficiency trade-off. Among the proposed variants, ShuffleFAC ($\gamma = 16$) achieves the best position in the accuracy-complexity space (Accuracy: $71.31 \pm 1.34\%$, F1: $71.45 \pm 1.18\%$) with only 39 K parameters and 3.06 M MACs, while achieving an inference latency of 6.05 ± 0.95 ms and an estimated energy of $15.14 \pm 2.37 \mu\text{Wh}$ on the Raspberry Pi. Notably, ShuffleFAC attains competitive accuracy with substantially lower model size and computational cost than conventional lightweight architectures. Across configurations, $\gamma = 8$ yields the lowest latency and energy, whereas increasing the width to $\gamma = 32$ achieves comparable accuracy; further scaling to $\gamma = 64$ increases compute and latency without improving performance. Overall, these results indicate that

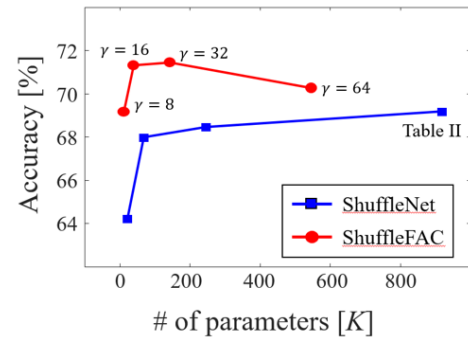


Fig. 3: Classification accuracy versus model size

ShuffleFAC is well suited for real-time UATR on resource-constrained platforms.

V. DISCUSSIONS

A. Comparison with Scaled ShuffleNet

ShuffleNet variants with different channel dimensions are compared to the corresponding ShuffleFAC variants under the same training and test protocol. Fig. 3 plots micro Accuracy versus the number of trainable parameters, where the upper-left region indicates a more favorable accuracy-model-size trade-off. As the ShuffleNet backbone is scaled down, its Accuracy degrades noticeably, indicating that the baseline becomes increasingly capacity-limited at small model sizes. In contrast, ShuffleFAC consistently achieves higher Accuracy than ShuffleNet at comparable parameter budgets. This improvement suggests that injecting frequency-position information helps compensate for the reduced capacity of lightweight backbones by enabling more discriminative feature extraction from time-frequency representations.

B. Embedded Inference Overhead Beyond MACs

Unlike a high-resource workstation equipped with parallel processors, an embedded platform typically relies on a single

CPU to execute the entire inference pipeline. As a result, the processor must handle not only core arithmetic (e.g., convolutions) but also auxiliary operations such as parameter loading, memory allocation, and tensor manipulation (e.g., copy, slice, and concatenation). MAC counts, however, account only for the core multiply-accumulate operations.

MicroNet0 achieves the lowest MACs by adopting micro-factorizing separable convolution. Profiling on a Raspberry Pi shows that MicroNet0 spends approximately 2.27 ms on tensor operations, accounting for about 15% of the total inference time, yet this overhead is excluded from MAC counts. When such tensor-manipulation overhead is non-negligible, measured embedded latency is not necessarily proportional to MACs, which is consistent with prior deployment-oriented observations (e.g., [10]) and related work on practical inference efficiency [13]. In contrast, ShuffleFAC ($\gamma = 16$) is designed to minimize tensor manipulation and spends only about 0.53 ms (approximately 9% of total time) on tensor operations. Because most of its runtime (about 82%) is dominated by core arithmetic, MACs provide a more reliable proxy for comparing computational complexity across ShuffleFAC variants.

C. Comparison with Recent Studies

Recent studies report UATR classification accuracies of around 96% [6], [16]. In those studies, segmented clips are randomly shuffled and then split into training and test sets. Under such segment-level partitioning, clips from the same source recording can appear in multiple subsets, so the model may be evaluated on test clips that are highly similar to recordings observed during training. In contrast, this study adopts a stricter recording-level split as described in Section IV-A. Consequently, all test clips originate from recordings that are never observed during training, providing a more reliable assessment of generalization to unseen ship-radiated sounds. In addition, this study prioritizes lightweight model design for resource-constrained deployment, which can further limit peak classification performance compared with heavier architectures.

VI. CONCLUSIONS

This letter introduces ShuffleFAC, a lightweight acoustic model for efficient ship-radiated sound classification in resource-constrained maritime monitoring systems. By integrating Frequency-Aware convolution with a channel-shuffling mechanism, the proposed model captures frequency-dependent acoustic patterns while maintaining a compact architecture with reduced computational cost. Experiments on the DeepShip dataset show that ShuffleFAC achieves competitive classification performance with substantially fewer parameters than existing lightweight models. Compared with MicroNet0, ShuffleFAC ($\gamma = 16$) improves the macro F1-score by 1.82 % (69.63 \rightarrow 71.45 %), reduces model size by $9.7 \times$ (379 \rightarrow 39 K), and achieves $2.5 \times$ faster inference (15.13 \rightarrow 6.05 ms) on Raspberry Pi platform. These results highlight its suitability for real-time deployment. Future work will focus on improving classification performance and validating the proposed model on additional datasets to further assess its generalization capability.

ACKNOWLEDGMENT

This research was supported by Basic Science Research Program through the National Research Foundation of Korea (NRF) funded by the Ministry of Science and ICT (RS-2024-00358953) and Korea Research Institute for Defense Technology planning and advancement(KRIT) funded by the Korea government (KRITCT-23-026)

REFERENCES

- [1] C. Gamage, R. Dinalankara, J. Samarabandu, and A. Subasinghe, "A comprehensive survey on the applications of machine learning techniques on maritime surveillance to detect abnormal maritime vessel behaviors," *WMU Journal of Maritime Affairs*, vol. 22, no. 4, pp. 447–477, 2023.
- [2] L. Bjørnø, "Underwater acoustic measurements and their applications," in *Applied underwater acoustics*. Elsevier, 2017, pp. 889–947.
- [3] M. Irfan, Z. Jiangbin, S. Ali, M. Iqbal, Z. Masood, and U. Hamid, "Deepship: An underwater acoustic benchmark dataset and a separable convolution based autoencoder for classification," *Expert Systems with Applications*, vol. 183, p. 115270, 2021.
- [4] L. Xin-xin, Y. Shi-e, and Y. Ming, "Feature extraction from underwater signals using wavelet packet transform," in *2008 International Conference on Neural Networks and Signal Processing*, 2008, pp. 400–405.
- [5] Z. Lian and T. Wu, "Feature extraction of underwater acoustic target signals using gammatone filterbank and subband instantaneous frequency," in *2022 IEEE 6th Advanced Information Technology, Electronic and Automation Control Conference (IAEAC)*, 2022, pp. 944–949.
- [6] S. Feng and X. Zhu, "A transformer-based deep learning network for underwater acoustic target recognition," *IEEE Geoscience and Remote Sensing Letters*, vol. 19, pp. 1–5, 2022.
- [7] A. G. Howard, M. Zhu, B. Chen, D. Kalenichenko, W. Wang, T. Weyand, M. Andreetto, and H. Adam, "Mobilennets: Efficient convolutional neural networks for mobile vision applications," *arXiv preprint arXiv:1704.04861*, 2017.
- [8] M. Sandler, A. Howard, M. Zhu, A. Zhmoginov, and L.-C. Chen, "Mobilennetv2: Inverted residuals and linear bottlenecks," in *Proceedings of the IEEE conference on computer vision and pattern recognition*, 2018, pp. 4510–4520.
- [9] X. Zhang, X. Zhou, M. Lin, and J. Sun, "Shufflenet: An extremely efficient convolutional neural network for mobile devices," in *Proceedings of the IEEE conference on computer vision and pattern recognition*, 2018, pp. 6848–6856.
- [10] N. Ma, X. Zhang, H.-T. Zheng, and J. Sun, "Shufflenet v2: Practical guidelines for efficient cnn architecture design," in *Proceedings of the European conference on computer vision (ECCV)*, 2018, pp. 116–131.
- [11] Y. Li, Y. Chen, X. Dai, D. Chen, M. Liu, L. Yuan, Z. Liu, L. Zhang, and N. Vasconcelos, "Micronet: Improving image recognition with extremely low flops," in *Proceedings of the IEEE/CVF International conference on computer vision*, 2021, pp. 468–477.
- [12] T. Song and W. Zhang, "Frequency-aware convolution for sound event detection," in *International Conference on Multimedia Modeling*. Springer, 2025, pp. 415–426.
- [13] C. Lee, W. Choi, and S. Park, "Hidden costs for inference with deep network on embedded system devices," in *Proceedings of the IEEE conference on consumer electronics*, 2025. [Online]. Available: <https://arxiv.org/abs/2601.01698>
- [14] H. Nam, S.-H. Kim, B.-Y. Ko, and Y.-H. Park, "Frequency dynamic convolution: Frequency-adaptive pattern recognition for sound event detection," *arXiv preprint arXiv:2203.15296*, 2022.
- [15] F. Chollet, "Xception: Deep learning with depthwise separable convolutions," in *Proceedings of the IEEE conference on computer vision and pattern recognition*, 2017, pp. 1251–1258.
- [16] S. Deng and F. Hong, "Advancing underwater acoustic target recognition in low-snr environments with uatr-diff-transformer," *Ocean Engineering*, vol. 341, p. 122668, 2025.